CAMD Studies of Coal Structure and Coal Liquefaction

Jean-Loup Faulon and Gary A. Carlson

Sandia National Laboratories, Fuel Science Department, Albuquerque, NM 87185-0710

Contract Number: 2181.000
Period of Performance: 10/89 - present
Objective: The purpose of this program is to use computer-aided molecular design (CAMD) techniques to increase our understanding of coal structure and its relationship to coal liquefaction.

1. Introduction

The macromolecular structure of coal is essential to understand the mechanisms occuring during coal liquefaction. Many attempts to model coal structure can be found in the literature. More specifically for high volatile bituminous coal, our subject of interest, the most commonly quoted models are the models of Given,[1] Wiser,[2] Solomon,[3] and Shinn.[4] In past work, we have used CAMD to develop three-dimensional representations for the above coal models.[5] The three-dimensional structures were energy minimized using molecular mechanics and molecular dynamics. True density and micopore volume were evaluated for each model. With the exception of Given's model, the computed density values were found to be in agreement with the corresponding experimental results.

The above coal models were constructed by a trial and error technique consisting of a manual fitting of the analytical data. It is obvious that for each model the amount of data is small compared to the actual complexity of coal, and for all of the models more than one structure can be built. Hence, the process by which one structure is chosen instead of another is not clear. In fact, all the authors agree that the structure they derived was only intended to represent an "average" coal model rather than a unique correct structure.

The first achievement of our work has been to propose a computer technique that automates the manual fitting between coal model and analytical data. We have developed[6] and used[7-9] a computer program (the SIGNATURE program) to produce bituminous coal models based solely on qualitative and quantitative experimental data. Besides building molecular structures, the SIGNATURE program estimates the number of possible models matching a given set of analytical data. For bituminous coal the number of possible models was found to be several hundred thousand. Since this number was too large to build all the models, we used a stochastic sampling technique to define an optimal subset of models which is an accurate representation of the entire population of possible models.[8]

To further characterize the structure of coal, our second achievement has been to develop a computer technique based on finite element theory that calculates physical characteristics of three-dimensional molecular models. More precisely, the technique computes the true density, the micropore volume, the surface area, and the fractal dimension of any given molecular model.[8,9] The technique has been applied with the coal models generated by the SIGNATURE program, and it was shown that the physical characteristics computed matched the corresponding experimental data. It was concluded that although there is a large number of

possible vitrinite models, a small subset of these models (e.g., 15) is sufficient to statistically represent this structure.[7,8]

The most recent achievement of our studies has been to couple our CAMD effort with kinetics modeling. We have modified the SIGNATURE program in order to apply chemical reactions to three-dimensional molecular models. The input of our kinetics program is a molecular model coupled with a reaction mechanism with associated rates. The output of the program is the molecular distribution of the products of the reactions. Our kinetics technique used the Monte Carlo stochastic method. We believe this new technique is more accurate than classical Monte Carlo kinetics programs, because our simulations are carried out in three-dimensional space. We have applied our kinetics program to investigate wood coalification, pyrolysis of coal, and are currently studying the effect of aromatic solvents in coal liquefaction.

2. Accomplishments

2.1 Modeling the macromolecular structure of coal

An important point needs to be mentioned regarding the utilization of CAMD for the study of coal. Prior to use of CAMD software, the connectivity (i.e. the structural formula) of the studied molecule has to be known. This information is unfortunately lacking for coal.

Many studies have been conducted in the past 25 years to resolve by computer the general problem of retrieving a structure from analytical data. The generic name for these studies is Computer-Assisted Structure Elucidation (CASE). We recently developed a new CASE technique (the SIGNATURE program) for the modeling of complex macromolecules. The technique is able to construct large molecular models from analytical structural data. Aside from constructing models in three-dimensional space, the SIGNATURE program is also able to compute the number of models possible. Knowledge of this number is crucial to our being able to decide how many models are necessary to represent coal. Even if this number is too large to allow all the models to be built, sampling theory makes it possible to select a subset of models (a sample) which is statistically representative of the whole population. Among the various techniques of sample design, the Simple Random Sampling Without Replacement (SRSWOR) is the most convenient to apply here.[8] The SIGNATURE program can directly build the required sample because the program permits the construction of non-identical random models.

The experimental material chosen for this report is a piece of coalified wood, specifically a fossil stem which was recovered from a lacustrine shale from the Midland Formation (Triassic) near Culpeper, Virginia. It is believed that this coalified wood sample is representative of vitrinite from HvC bituminous coal.[10] The analytical data supplied to the SIGNATURE program are summarized in Table I. The SIGNATURE program was run and all the solutions containing 333 carbon atoms were searched. This number of carbons was chosen considering the computational time and the fact that all the fragments listed in Table I must be present in the models. The SIGNATURE program found only five different molecular formulas (Table II) having a deviation between model and analytical data less than 1%.

In our first attempt to construct realistic models of coal structure, the SIGNATURE program was asked to build one random structure for each of the solutions listed in Table II. Then, structural, energetic, and physical characteristics were calculated for each of the five constructed models. The results we obtained clearly demonstrated that the five structures constructed did not match experimental results. First, the number averaged molecular weight of

the clusters (M_o = 77 amu) and the number averaged molecular weight between branch points (M_c = 61-65 amu) did not match the values reported using swelling experiments (for M_o < 100 amu, M_c > 200 amu).[11] Second, the potential energy was at least 25 times larger than values reported by other CAMD studies of bituminous coal.[5] Third, the helium density (1.43-1.52 g/cc) was too high compared to the experimental values reported for vitrinite from HvC bituminous coal (1.25 - 1.30 g/cc).[12] Finally, there were no micropores in the models constructed.

As shown in Table I, the fragments which form the models are mainly alkylbenzenes and alkylphenols. It is clear that these types of fragments, when randomly connected, generate highly cross-linked structures. The only possible way of decreasing the cross-link density with such a system is to increase the size of the clusters. In order to increase the size of the clusters one needs to merge the pyrolysis fragments into larger sub-structures such as hydroaromatic sub-structures. There is no direct evidence that hydroaromatic clusters exist in bituminous coal, but there is some indirect support from liquefaction experiments.[4] Figure 1 depicts an example of construction of hydroaromatic clusters from pyrolysis fragments.

Considering all of these previous observations, the SIGNATURE program was set up to build models by forming the maximum number of five or six membered rings. The purpose of this constraint was to generate larger clusters from the initial molecular fragments. The stochastic structure generator estimated that the number of possible models was equal to 319 318. As presented in Table II, the population of possible coal models is subdivided into five different C_{333} structures. To build a sample which is a good representation of the entire population, the sample size of each C_{333} structure has to be proportional to the corresponding population of all of its possible isomers. Considering the population size of each C_{333} structures and the computational time required to build the structures and evaluate the different characteristics, we chose to build a sample of 15 structures comprising the following: 2 structures of $C_{333}H_{302}O_{16}$, 10 structures of $C_{333}H_{304}O_{16}$, 1 structure of $C_{333}H_{306}O_{16}$, 1 structure of $C_{333}H_{308}O_{16}$, and 1 structure of $C_{333}H_{310}O_{16}$. To find the minimum energy conformation of each model, the structures were submitted to molecular mechanics and dynamics simulations, using the computational methods provided by POLYGRAF software (Molecular Simulation Inc.). Molecular mechanics were used to find the closest minimum for the potential energy starting from an initial conformation. The potential energy was calculated using the DREIDING force field[13] and minimized using the classical conjugate gradient and steepest descents algorithms. In the physical world molecules find their global minimum energy conformation by fluctuating about several configurations within energetic reach, as determined by the system temperature. These fluctuations can be computer-simulated by what is called molecular dynamics. In the present study, the time step chosen for all molecular dynamics calculations was 1 fs and the dynamics simulations were performed for 60 ps at a constant 300 K temperature. It was observed that 60 ps was enough to locate a global minimum of energy. For all the structures the energy decreased only during the first 30 ps of the dynamics simulation and then remained approximately constant. The minimized energies of the sample of 15 C_{333} coal models are listed in Figure 2a.

2.2 Computing the physical properties of coal macromolecular structures

The helium density, the closed porosity volume, the micropore volume, the surface area, and the fractal dimension are the physical characteristics measured for our coal molecular models.

All these characteristics were calculated for energy minimized conformations. The conformations were obtained as described in section 2.1.

2.2.1 Helium density

The true density of a porous structure is the mass of a unit volume of the pore-free structure. Experimentally, the true density of coal is approximated using helium pycnometry. It is thus more appropriate to employ the term "helium density". We computer-simulated the calculation of the helium density by immersing the structure in a grid (of volume V_G) composed of cubic cells of 0.1 nm length. Briefly, the helium density is determined by dividing the molecular weight of the structure (MW) by the volume of the structure (V_s^{He}) and multiplying the result by Avogadro's number. The volume V_s^{He} is the volume not accessible to helium atoms and is the volumetric sum of three regions defined as *atomic* cells, *internal* cells, and *closed* cells (Figure 3). An atomic cell is a cell included in the Van der Waals sphere of any atom. The sum of the volume of all atomic cells defines the atomic volume. Internal cells are cells not accessible to helium atoms because they are located between two or more atoms having an inter-atomic distance less than a critical value. The critical distance has been defined by Walker and co-workers[14] as the sum of the kinetic diameter of the diffusing species plus 0.16 nm. Recently, Rao[15] has calculated this critical size from the diffusion of different gases though carbon micropores. The values were determined using a Lennard-Jones (6-12) function to represent the atom-atom interactions. The critical value calculated for helium is 0.508 nm. Considering this result, we define an internal cell as a cell located between two atoms having an inter-atomic distance less than 0.508 nm. The sum of all internal cells defines the internal volume. Closed cells are determined after determining atomic and internal cells, and represent closed volumes (i.e. cells surrounded by atomic and internal cells). The sum of all closed cells defines the closed porosity volume. Since closed cells are not accessible to helium, they must be included in the volume V_s^{He} when we are calculating the helium density and comparing it to experimentally determined values. The helium densities of the 15 C_{333} coal models are depicted in Figure 2b.

2.2.2 Micropore volume

Microporosity is defined according to the method of Gan *et al.*[16] The micropore volume (V_3) is the volume of pores having a diameter less than 1.2 nm, and is defined by the following equation:

$$V_3 = V_T - (V_1 + V_2) \quad (1)$$

where V_T is the total pore volume accessible to helium, V_1 is the volume of pores having a diameter greater than 30 nm, and V_2 is the volume of pores ranging between 1.2-30.0 nm in diameter. In our computer model, V_T is equal to the difference between the volume of the grid (V_G) and V_s^{He}. Thus,

$$V_T = V_G - V_s^{He} \quad (2)$$

Our models are generally smaller than 30.0 nm, therefore, the volume V_1 is set to zero. The volume V2 is determined using the grid method and a critical distance equal to 0.572 nm. This value, determined by Rao,[15] is the critical distance for diffusion of nitrogen molecules through carbon micropores. Hence, V_2 is equal to the difference between the total volume of the grid and the volume of the structure not accessible to nitrogen molecule ($V_s^{N_2}$):

$$V_2 = V_G - V_s^{N_2} \quad (3)$$

By substituting equations 1 and 2 into 3 we obtain the following relationship defining the computer simulated micropore volume:

$$V_3 = V_s^{N_2} - V_s^{He} \quad (4)$$

The procedure used to calculate V_3 is visually depicted in Figure 4. The micropore volumes of the 15 C_{333} coal models are listed in Figure 2c.

Equation 4 calculates the micropore volume of pore accessible to He but not accessible to N_2. In other words, V_3 is the pore volume of micropore having an entrance size between λ_1 = 0.508 nm and λ_2 = 0.572 nm. Hence, by varying the values of λ_1 and λ_2 the procedure depicted in Figure 4 can be used to calculate the micropore volume distribution. Figure 5 gives the average micropore volume distribution of our 15 C_{333} coal models.

2.2.3 Surface area and fractal dimension

Experimentally, a number of techniques exist to measure surface areas and pore volumes of coals. The most common techniques are based on adsorption of gases. Surface areas measured using adsorption of gases differ depending on the sizes and shapes of the adsorbate molecules used, and the temperature and pressure of adsorption. The surface areas also depends on the adsorbate/adsorbent specific interactions. Evidence for the influence of the adsorbate molecule on the surface area of coals is shown by the different results obtained when measuring the surface area with N_2 and CO_2.[17] However, the BET and the Polanyi-Dubinin calculation with CO_2 are thought to provide the most meaningful value for coals.[17]

As for the density and the micropore volume, the surface area is computer-simulated by placing the three-dimensional structure within a three dimensional grid. We define two types of surface area - the total surface area, and the pore surface area. The total surface area represents the actual surface of the structure. Since atomic and internal cells are inaccessible to adsorbate molecules, the total surface area is computed by summing all the areas of cell faces between an *atomic* or *internal* cell and a *non-atomic* or *non-internal* cell (not including *closed* cell). The pore surface area is the surface of the micropore volume. The pore surface is the sum of the areas of all faces that are between a *micropore* cell (cf. Figure 4) and an *atomic* or an *internal* cell (not including *closed* cell).

The surface areas of the 15 C_{333} coal models were calculated using the above procedure. The calculated total surface area for all of the models was found at least 10 times larger than the values measured by CO_2 absorption,[17] and about 100 times larger than the BET surface area obtained with N_2 for the same rank of coal.[17] However, the calculated total surface area should not be compared with experimental results because the sizes of our models are small and the external surfaces (surfaces of the boundaries of the structures) are much larger than the internal surfaces (surfaces of the micropores). This contrasts with experimental results, where the external surface area is negligible compared to the internal surface area for macroscopic particle size. Since experimentally the micropore surface area is dominant, we should expect our micropore surface calculation to be in better agreement with experimental results. We indeed found the micropore surface areas calculated for our models relatively close to the CO_2 surface area measured for HvC bituminous coal (100-200 m^2/g).[17] Nevertheless, our mean value (291 m^2/g) was slightly larger than experimental values. Our calculations were performed using a cell grid size of 0.1 nm length. The same calculations made with a cell grid size of 0.2 nm gave an average micropore surface area of 190 m^2/g. As we will see in the following, the influence of the grid size used to measure the micropore surface area can simply be explained using fractal theory.

It is known that the surface area of coal behaves like a fractal surface;[18] therefore, an increase in the cell size should lead to a decrease in the surface area. Pfeifer and Avnir[19]

demonstrated that if N is the number of adsorbate molecules covering the surface and r is the radius of the adsorbate molecule,

$$N \sim r^{-D} \tag{5}$$

where D is the fractal dimension of the surface of the studied structure. When applied to our models, the same relationship should apply if N is the number of cell faces which belong to the micropore surface and r is the size of the cells. Figure 6a shows clearly that a log-log plot of N versus r is linear. Therefore, the micropore surface of the model $C_{333}H_{302}O_{16}$ is a fractal surface having a dimension D = 2.68 (i.e. the negative slope of the curve plot in Figure 6a).

Prior to calculating the fractal dimension of the micropore surface area, it is necessary to compute the micropore volume. This two steps calculation generates numerical errors. When we applied this calculation to our 15 models, we found large differences between the fractal dimensions of the micropore surface areas, and our results were statistically meaningless.

If the micropore surfaces of our models are indeed fractal surfaces, we should expect the total surface of our models to be fractal surfaces. Even though the total surface has no physical significance, the total surface includes the micropore surface, and the fractal dimension of the total surface should be equal to the fractal dimension of the micropore surface. Calculating the fractal dimension directly from the total surface allows one to avoid the determination of the micropore volume; consequently, this calculation is more straightforward and minimizes the numerical errors.

The fractal dimensions of the total surface areas for all the 15 models were calculated using equation (5), with r varying between 0.1 nm and 0.8 nm. The results are presented in Figure 6b. The average fractal dimension is 2.71 and the population deviation calculated using our sampling technique[8] is only 0.05. Thus, from the slopes of the curves plotted in Figures 6 a and b, we can conclude that the fractal dimensions of the total surface area and the micropore surface area are almost identical.

It is important to point out that the fractal dimension and the micropore volume distribution can be used to predict the surface area obtained for a given adsorbate molecule. Consider an adsorbate molecule of average radius r and cross-section area σ. Let ρ be the smallest pore radius which can be accessed by the adsorbate molecule. Let S be the micropore surface area measured with the adsorbate molecule. Let $S_1(\rho)$ be the micropore surface area obtained from Figure 5-b; $S_1(\rho)$ is the surface area of micropores having a radius larger than ρ calculated using the grid system with cells of length equal to r = 0.1 nm. By replacing in equation (I) the number of moles of adsorbate molecule (N) by S/σ, and r by $\sigma^{1/2}$, we obtain

$$S \sim \sigma^{1-D/2} \tag{6}$$

equation (6) can be written in the form

$$S \sim S_1(\rho)\, \sigma^{1-D/2} \tag{7}$$

According to Rao,[15] CO_2 can access all the pores having a radius greater than 0.271 nm. The corresponding surface area calculated from Figure 5-b is therefore about 300 m^2/g. At room temperature the cross-section area of CO_2 is $\sigma = 20.5$ Å^2 [20]. Application of equation (7) with D = 2.71 yields a micropore surface area of 103 m^2/g if CO_2 is the adsorbate molecule. This value is in the range of experimental results for HvC bituminous coal (100-200 m^2/g).[17]

The above calculations performed for CO_2, cannot be done for N_2 because it is not clear from the literature which pore sizes N_2 can penetrate. Rao[15] calculated that N_2 can access all the pores in carbon structures having a radius larger than 0.286 nm, but Gan et *al.*[16] assumes that N_2

at -196^{0}C cannot penetrate pores having a radius less than 0.6 nm. Equation (7) can provide an answer to this discrepancy. The surface area measured using N_2 at -196 ^{0}C for HvC bituminous coal is about 10 m^2/g [17] and the cross-section area σ = 16.2 Å^2 [21]. Plugging the previous values into equation (7) gives $S_1(r) = 27$ m^2/g for D = 2.71, and the corresponding pore radius obtained from Figure 5-b is $\rho = 0.46$ nm. Therefore, according to our results N_2 cannot penetrate pores having a diameter lower than 0.92 nm. Figure 7 displays the micropore volumes accessible for CO_2 (Fig. 7-c) and N_2 (Fig. 7-d) for the first model of the sample ($C_{333}H_{302}O_{16}$). The diameter found for N_2 (0.92 nm) is only approximate due to the population deviation of the fractal dimension; however, we can state, that if there is adsorption phenomenon with both CO_2 and N_2 when measuring coal surfaces of HvC rank, only CO_2 penetrates the ultramicropores.

2.3 Statistical interpretation

All 15 of the C_{333} models match well with the quantitative analytical data with an average deviation of less than one percent. The cross-link densities found (Figure 2) are a direct consequence of the analytical data. The number averaged molecular weight of our coal clusters is 455.6 amu. The number averaged molecular weight between branch points averages 1057 amu. These values agree well with swelling experiments for acetylated and pyridine extracted bituminous coal (when 330 amu < M_o < 580 amu, 1000 amu < M_c < 1160 amu).[11] Furthermore, the average number of clusters between branch points (2.3) is in the range of values obtained from swelling experiments (2-4 clusters between branch points when the weight percentage of carbon is greater than 85).[22]

The computed helium density averages 1.26 g/cc for all 15 C_{333} structures constructed and the population deviation is less than 2 percent of this value. This result is in good agreement with experimental results found for vitrinite at a rank of bituminous coal (1.25 - 1.30 g/cc).[12] The closed microporosity is almost non-existent for most of the 15 models and is lower than 7% of the total micropore volume. The computed micropore volume averages 0.030 cc/g with a population deviation of 13 percent. The micropore volume is slightly lower than experimental values found for HvC bituminous rank (0.039 - 0.070 cc/g).[16] The low microporosity may be due to the size of our models; they are rather small compared to the particle sizes used in porosimetry experiments. Finally, the average fractal dimension 2.71 found for the 15 C_{333} structures agrees well with SAXS experimental values obtained for high vitrinite content bituminous coal.[18e]

One important result of this study is the micropore size distribution given in Figure 5. This presents for the first time, quantitative data regarding the ultramicroporous structure of bituminous coal. Such information cannot be obtained from experimental results due to the difficulty in measuring ultramicropore volumes (micropore volumes having a diameter less than 0.8 nm). Nevertheless, the fact that the micropore distribution is compatible with the fractal dimensionality of coal (obtained from both model and experiment) suggests that the distribution proposed is accurate. According to Figure 5 we can see that the smaller the micropore entrance size, the larger the corresponding micropore volume. We can also notice that most of the micropores are ultramicropores.

In summary, all the characteristics that we have calculated agree well with experimental data. Further, the energetics and physical characteristics found for the different models are relatively close to each other and the variances are small. In order to match all the analytical data,

our statistical results demonstrated that the number averaged molecular weight between branch points (M_c) is greater than 559 amu. However, no upper limit was found for M_c. These observations suggest that each model is in itself a reasonable representation of vitrinite including the model which does not contain covalent cross-links (structure $C_{333}H_{310}O_{16}$).

2.4 Kinetics modeling

In the previous sections, we have used the SIGNATURE program to generate three-dimensional molecular models from analytical data. To construct molecular models the SIGNATURE program assembles molecular fragments using interfragment bonds. Therefore, the main task achieved during the process of construction is the creation of bonds. Chemical reactions can be described by a succession of bonds that are created and/or broken. Hence, the SIGNATURE program can handle chemical reactions if we add the possibility of breaking bonds. We have modified the SIGNATURE program in order to apply reaction mechanisms to three-dimensional molecular models. The general scheme of our kinetics program is as follows:

a) The user inputs the chemical reactions in the form of molecular files. Each reaction file contains the atoms participating in the reaction. The bonds that are broken or created during the reaction are marked. For each reaction the user inputs the rate constant and the order of the reaction.

b) The reaction mechanism is applied by the SIGNATURE program on a given three-dimensional molecular model using the Monte Carlo method. More precisely, for each reaction the program searches all the sites in the molecular model that match the corresponding reaction file. The sites must be composed of the same atom types and bond types as the reaction file (topological matching) and the relative positions of the atoms must be the same in the molecular model as in the reaction file (geometrical matching).

c) For each site of the molecular model found to match the reaction files, a Monte Carlo process is applied. This is accomplished by comparing a random number (RN) versus the reaction probability. For example, the exact form of the probability that a site in state A will undergo a transition to state B in a time *dt* for a first-order irreversible reaction process is given in equation (8)

$$P = 1 - e^{-k\,dt} \tag{8}$$

where k is the rate constant of the reaction A $\longrightarrow$ B. If RN $< P$, the site being tested for the reaction undergoes the transition. If RN $\geq P$, the site does not react.

d) The program outputs the products distribution at each step *dt* of the Monte Carlo process.

In order to test our kinetics program we chose to model coal devolatization. Coal devolatization has already been studied using Monte Carlo[23] and percolation theories.[24] It has been shown that both techniques give similar results and match well experimental data.[25] There are two main differences between previous works and the current one.

a) The previous models represent the structure of coal by a network composed of monomers connected by bridges. The only information introduced regarding the monomers is their average molecular weight, and there are only two types of bridges: breakable and unbreakable. In the current study the coal models we used during the kinetics simulation have

been constructed by the SIGNATURE program using experimental structural analytical data. Therefore, these models are composed of all the atom types and all the bond types present in coal.

b) Our models and simulations take place in three-dimensional space while the previous models and simulations are dimensionless.

According to Solomon *et al.*[23] there are two main reactions occuring during coal devolatilization, bridge breaking and cross-linking. The reactions are assumed to be first-order irreversible. Like Solomon *et al.*,[23] Grant *et al.*,[24a] and Fletcher *et al.*[24b] we have assumed a single rate for the two main reactions, although in principal bridge breaking and cross-linking are composed of several reactions each having a different rate. Using the rates taken from ref. 23 , we ran a series of simulations with the 15 C_{333} coal models. Results are presented in Figure 8. The curve obtained for high cross-linked coal network (i.e., $M_c = 569$ amu) match well the experimental results obtained by Serio *et al.*[26] and the simulations results obtained by Grant *et al.*[24a] and Fletcher *et al.*[24b] This is not surprising considering that $M_c = 569$ amu corresponds to a coal network having an average number of bridges per cluster equal to 2.7, which is the value taken by the previous authors for bituminous coal. Hence, our simulations seem to indicate that bituminous coal is a high cross-linked polymer network.

3. Conclusions

The most important conclusion of the present work is that we have been able to develop a technique that uses the power of the computer to create a number of molecular models for coal using actual quantitative and qualitative experimental data, and to show that the models, from a statistical viewpoint, are a good representation of the coal structure. Previous attempts at definitions of coal molecular structure, including previous computer models, necessarily included investigator bias and could not be proven to be representative or average coal structures. In the present study, we can conclude that for the physical properties investigated, a sample of 15 structures is sufficient to represent statistically the whole population of vitrinite from HvC bituminous.

The results of our kinetics simulations are similar to the previously published results obtained using Monte Carlo[23] and percolation theories.[24] However, in all of these calculations, it was assumed that there are only two main reactions occurring during coal devolatilization. A better modeling would be obtained if we were able to incorporate in the devolatilization reaction mechanism all the atom types and bond types present in coal. We are currently investigating how to use *ab initio* calculations to derive the transition states and the activation energies of the possible chemical reactions that may occur in coal devolatilization and coal liquefaction. We are also studying how to use molecular dynamics and statistical mechanics to estimate the preexponential factors in the Arrhenius equations of the above reactions.

Since coal is a highly heterogeneous and complex material, it is not possible to study its structure and its reactivity using classical deterministic computational technique. However, the present work demonstrates that efficient stochastic techniques can be designed to analyze the structure and reactivity of coal. These techniques are now being ported to the massively-parallel computers at Sandia National Laboratories, which will allow much larger simulations to be studied.

References

1. Given, P. H., *Fuel* **1960**, *39*, 147.
2. Wiser, W. H. *NATO ASI Series C* **1983**, *124*, 325.
3. Solomon, P.R. *New Approaches in Coal Chemistry*, ACS Symposium Series No. 169; American Chemical Society: Washington, DC, 1981; pp 61.
4. Shinn, J. H. *Fuel* **1981**, *63*, 1187.
5. (a) Carlson, G. A. *Prepr. Pap. - Am. Chem. Soc. Div. Fuel Chem.* **1989**, 34(3), 780. (b) Carlson, G. A.; Granoff B. In Coal Science II: Schobert H. H., Bartle, K. D. Eds., ACS Symp. Ser. 461, Washington, DC, 1991, pp. 159. (c) Carlson, G. A. *Energy Fuels* **1992**, *6*, 771.
6. (a) Faulon, J. L. *J. Chem. Inf. Comput. Sci.* **1992**, *32*, 338. (b) Faulon, J. L. *J. Chem. Inf. Comput. Sci.* **1994**, *in press.*
7. Faulon J. L.; Hatcher P. G.; Carlson, G.A.; Wenzel, K. A. *Fuel Processing Technology* **1992**, *34*, 277-293.
8. Faulon J. L. ; Carlson G. A.; and Hatcher P. G. *Energy & Fuels* **1993**, *7*, 1062-1072.
9. Faulon J. L.; Mathews J. P.; Carlson G. A.; Hatcher P. G. *Energy & Fuels* **1994**, *8*, 408-414.
10. Hatcher, P. G.; Faulon, J. L.; Wenzel, K. A.; Cody, G. D. *Energy Fuels* **1992**, *6*, 813.
11. Larsen, J. W.; Green, T. K.; Kovac, J. *J. Org. Chem.* **1985**, 50, 4729.
12. Crelling, J. C. *Proc 1987 Int. Conf. Coal Sci.* **1987**, 119.
13. Mayo, S. L.; Olafson, B. D.; Goddard, W. A. *J. Phys. Chem.* **1990**, *94*, 8897.
14. Walker, P. L., Jr.; Austin, L. G.; Nandi, S. P. In Chemistry and Physics of Carbon: Walker, P. L., Jr., Ed., Marcel Deker: New York, NY, 1966; Vol. 2, pp. 257-371.
15. Rao, M. B. *Carbon* **1991**, *29*, 813.
16. Gan, H.; Nandi, S. P.; Walker, P. L., Jr. *Fuel* **1972**, 51, 272.
17. Mahajan, O. P. Coal Porosity In Coal Structures; Meyers, R. A., Ed.; Academic Press: New York, NY, 1982; pp 51-86.
18. (a) Larsen, J. W.; Wernet, P. C. *Prepr. Pap.- Am. Chem. Soc. Div. Fuel Chem.* 1992, **37(2)**, 849. (b) Bale, H. D.; Schmidt, P. W. *Phys. Rev. Lett.* 1984, **53**, 596. (c) Reich, M. H.; Snook, I. K.; Wagenfeld, H. K. *Fuel* 1992,**71**, 669. (d) Reich, M. H.; Russo, S. P.; Snook, I. K.; Wagenfeld, H. K. *J. of Colloid Interface Sci.* 1990, **135**, 353. (e) Wernett, P. C. *Characterization of the Pore Structure of Coals* . PhD Thesis, Lehigh University, Lehigh, 1991. (f) Friesen, W. I.; Mikula, R. J. *J. of Colloid Interface Sci.* 1987, **120**, 268.
19. Pfeifer, P.; Avnir, D. *J. Chem. Phys.* 1983, 79, 3558.
20. Walker, P.L; Kini, K. A. *Fuel* 1965, **44**, 453.
21. Emmett, P. H.; Brunauer, S. *J. Am. Chem. Soc.* 1937, **59**, 2682.
22. Lucht, L. M.; Peppas, N. A. *Fuel* **1987**, 66, 803.
23. Solomon, P. R.; Hamblen, D. G.; Yu Z. Z.; Serio, M. *Fuel* **1990**, 69, 754.
24. (a) Grant, D. M.; Pugmire R. J.; Fletcher, T. H.; Kerstein A. R. *Energy & Fuels* **1989**, *3*, 175. (b) Fletcher, T. H.; Kerstein, A. R.; Pugmire R. J.; Solum, M. S.; Grant, D. M. *Energy & Fuels* **1992**, *6*, 414.
25. Solomon, P. R.; Fletcher, T. H.; Pugmire, R. J. *Fuel* **1993**, 72, 587.
26. Serio, M. A.; Hamblen, D. G.; Markham, J. R.; Solomon, P. R. *Energy & Fuels* **1987**, *1*, 138.

Acknowledgments
Funding was provided by the US. Department of Energy at Sandia National Laboratories under contract DE-AC04-94AL8500. We thank Dr. P. G. Hatcher from the Pennsylvania State University for many helpful discussions.

Table I. Analytical data for HvC Bituminous coalified wood (Midland Stem, ref. 10).

Parameter	Analytical Data	Model ($C_{333}H_{302}O_{16}$)	Deviation Analytical data - Model
Elemental analysis and carbon-13 NMR data (normalized for 100 carbon atoms)			
C	100.0	100.0	-
H	92.0	91.8	0.2
O	5.0	4.6	0.4
f_a (aromatic carbon)	62.5	63.0	-0.5
f_a^H (protonated aromatic carbon)	28.0	27.6	0.4
f_a^P (phenolic or phenolic ether)	7.5	7.5	0.0
f_{al} (aliphatic carbon)	37.5	37.4	0.1
f_{al}^H (aliphatic CH or CH_2)	26.0	26.2	-0.2
f_{al}^* (aliphatic CH_3)	11.5	11.2	0.3
Average deviation			± 0.26
Flash Pyrolysis/gc/ms data (weight % normalized to total aromatic fragments)			
benzene	3.3	2.0 (1)	1.3
toluene	4.8	4.8 (2)	0.0
C-2 benzenes	5.2	8.3 (3)	-3.1
C-3 benzenes	3.9	6.3 (2)	-2.4
phenol	3.6	2.5 (1)	1.1
o -cresol	5.7	2.8 (1)	2.9
m + *p* -cresol	13.0	8.5 (3)	4.5
2,4 dimethylphenol	12.0	9.6 (3)	2.4
other C-2 phenols	10.3	6.4 (2)	3.9
C-3 phenols	10.9	14.2 (4)	-3.3
C-4 phenols	4.8	3.9 (1)	0.9
alkylnaphthalenes	17.0	24.4 (6)	-7.4
alkyldibenzofurans	5.2	6.2 (1)	-1.0
methyl	-	(7)	
ethyl	-	(9)	
propyl	-	(3)	
C4-C22	-	(0)	

Values in parentheses are the quantities of each fragment corresponding to a molecule containing 333 carbon atoms.

Table II. Deviation analytical data - model and population information for each of the C_{333} molecular formula[a]

Molecular Formula	Average deviation[b]	Number of possible models
$C_{333}H_{302}O_{16}$	0.26	52,272
$C_{333}H_{304}O_{16}$	0.29	231,000
$C_{333}H_{306}O_{16}$	0.39	24,750
$C_{333}H_{308}O_{16}$	0.49	9,856
$C_{333}H_{310}O_{16}$	0.71	1,440

[a] The numbers of possible models have been estimated using the isomer generator provided by the SIGNATURE program.[b] The deviation is the average deviation between model and quantitative analytical data as calculated in Table I.

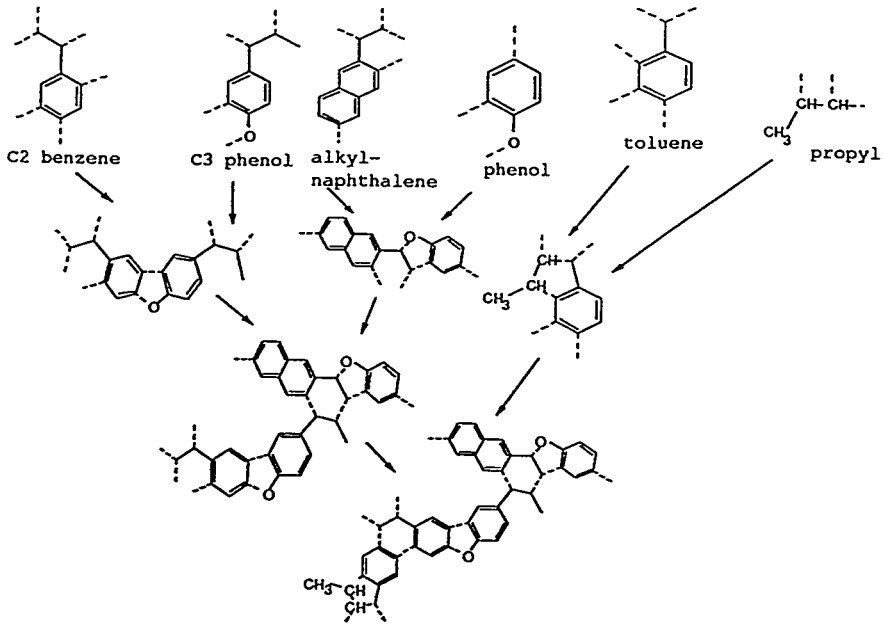

Figure 1. An example depicting the construction of a hydroaromatic cluster.The initial fragments (top of the figure) are fragments identified by pyrolysis/gc/ms analysis.

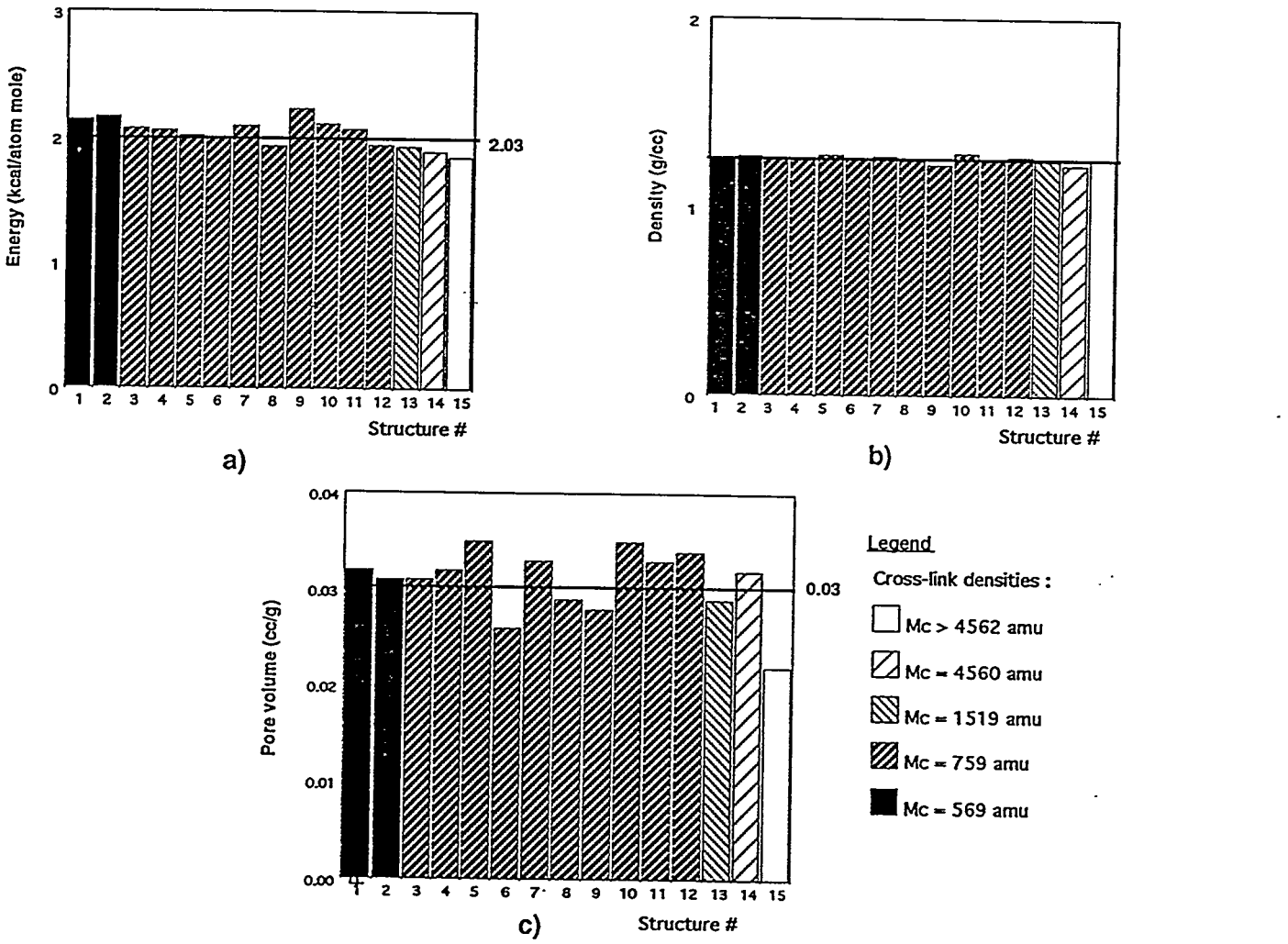

Figure 2. Correlation between physical characteristics and cross-link densities for each of the 15 individual models comprising the sample. For each graph, the horizontal line represents the population mean.

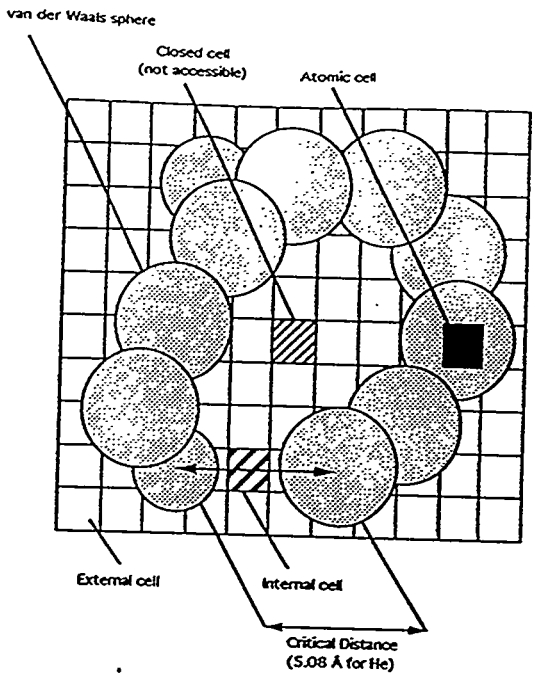

Figure 3. 2D projection of the grid system used to calculate helium density. The disks are the projections of the van der Waals spheres for the atoms. The double arrow represents the critical distance which defines internal cells.

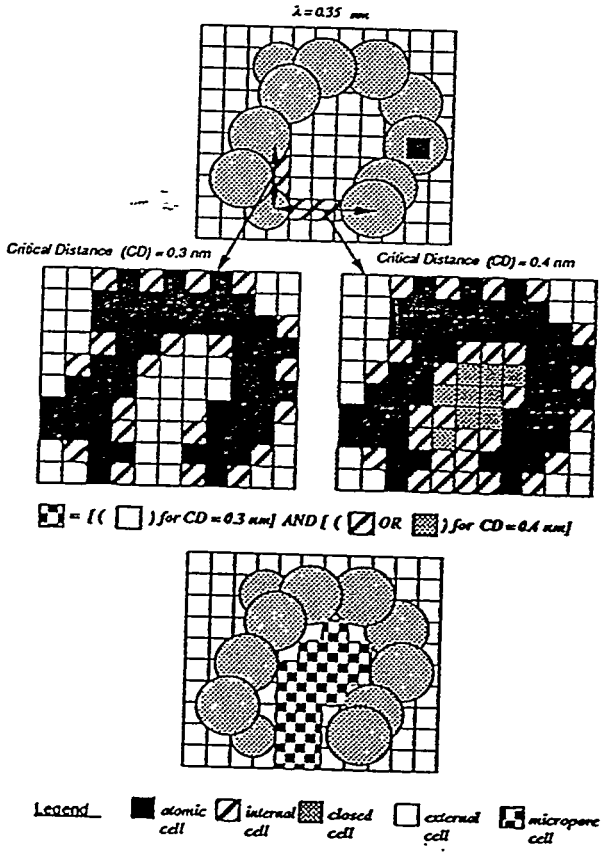

Figure 4. Schematic 2D projection representing the calculation of the micropore volume.

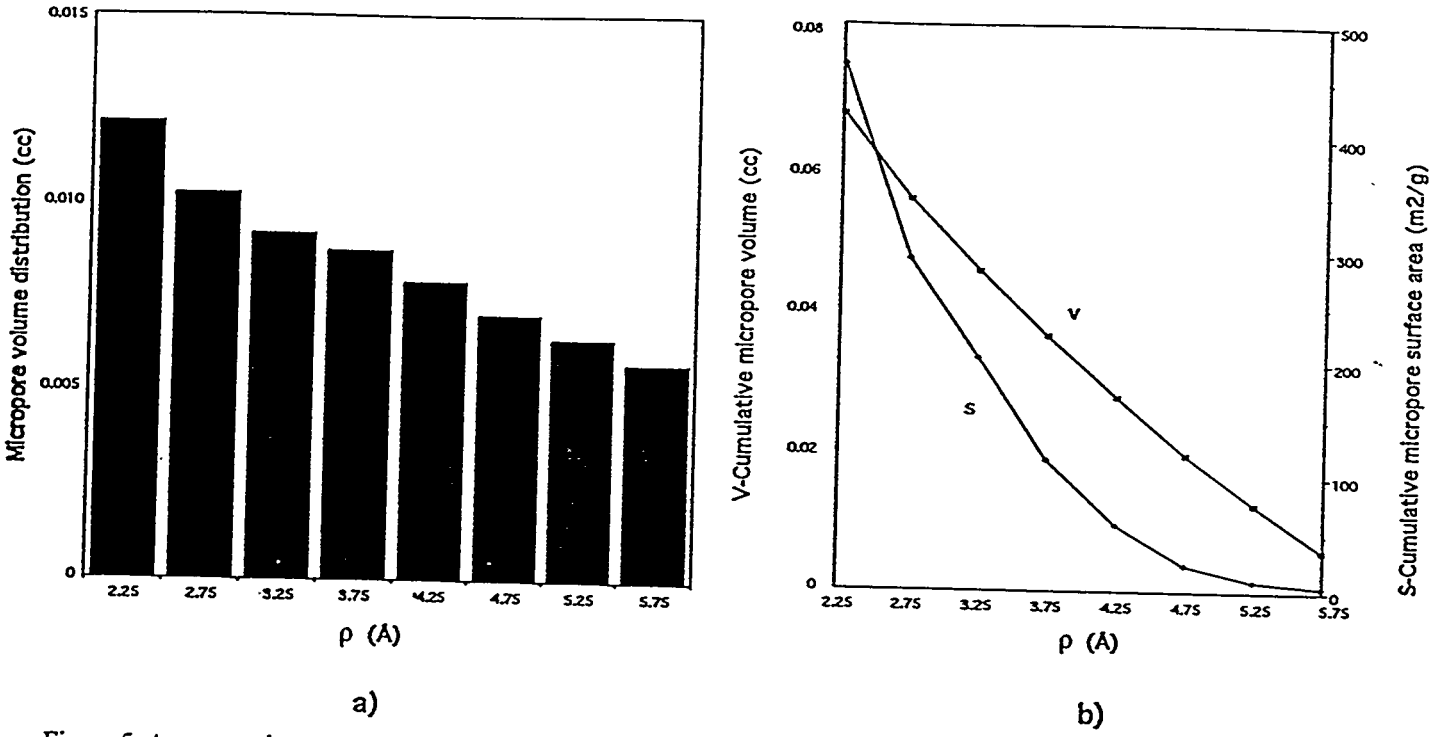

Figure 5. Average micropore volume distribution and micropore surface area for the 15 models. a) This figure represents the micropore volume versus the micropore radius (r). The pore entrance size ($l = 2\,r$) varies from 0.45 ± 0.05 nm to 1.15 ± 0.05 nm. b) Curve V is the cumulative micropore volume having a pore radius r varying from 0.225 nm to 0.575 nm. Curve S is the corresponding micropore surface area. Micropore volumes and surfaces areas were calculated using a cell size of 0.1 nm.

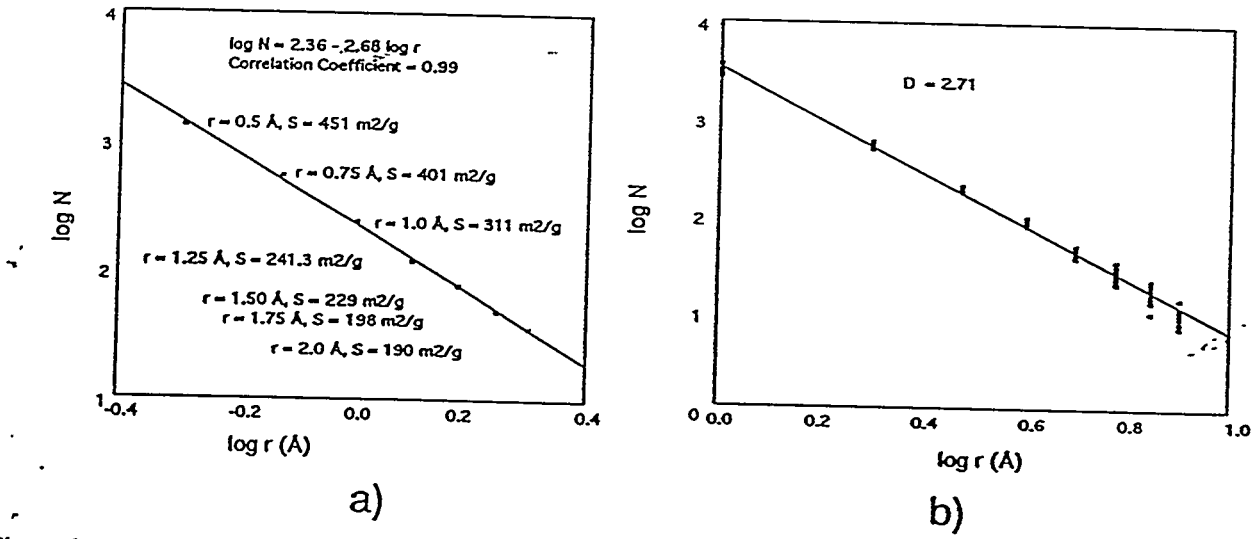

Figure 6. a) Micropore surface areas for the model $C_{333}H_{302}O_{16}$. b) Fractal dimension for the 15 models obtained by varying the sizes of the cells . Both figures plots on a log-log scale the number of cell faces (N) which belong to the micropore surface (a) and total surface (b) versus the size of the cells (r).

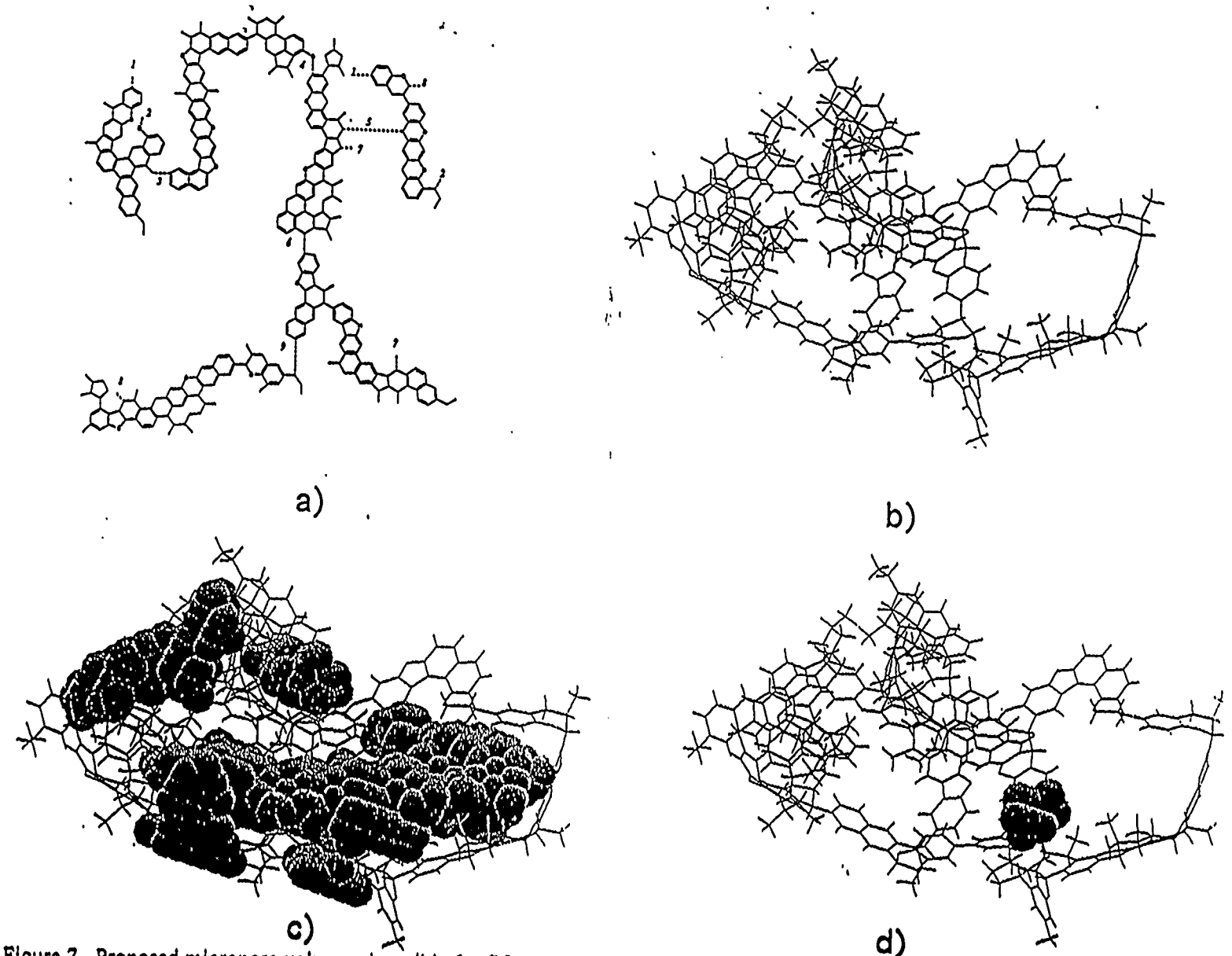

Figure 7. Proposed micropore volume accessible for CO_2 and N_2. (a) Structural formula of the first model of the sample ($C_{333}H_{302}O_{16}$). (b) Corresponding energy-minimized 3D structure. (c) Micropore volume accessible by CO_2 represented by solid spheres (of 0.1 nm radius) centered on the cubic cells. (d) Micropore volume accessible by N_2 at 77 K.

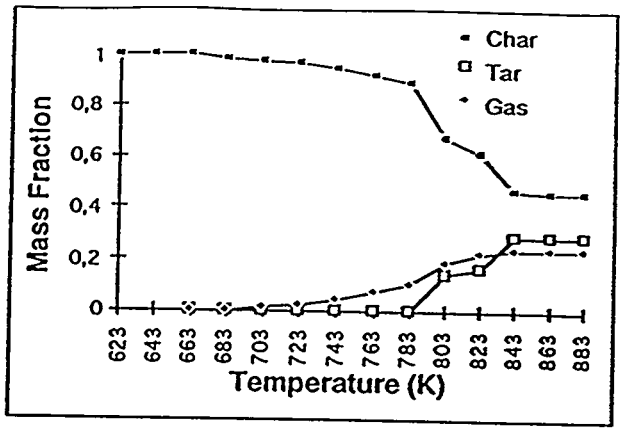

Mc = 569 amu

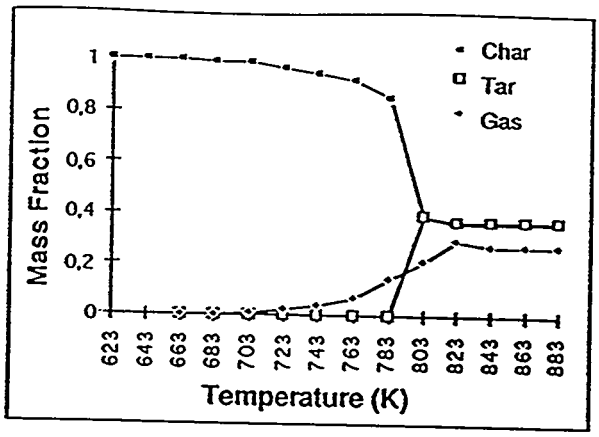

Mc = 759 amu

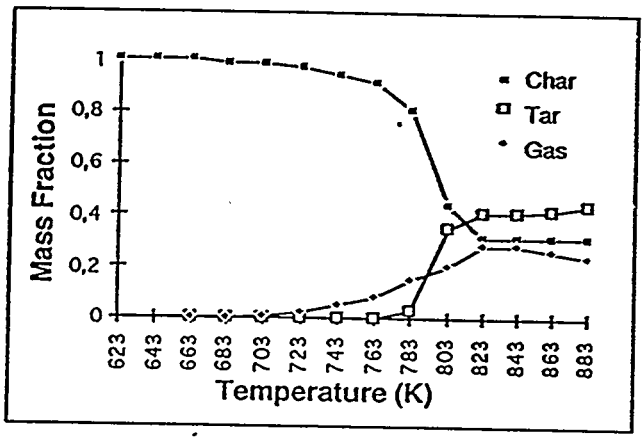

Mc = 1519 amu

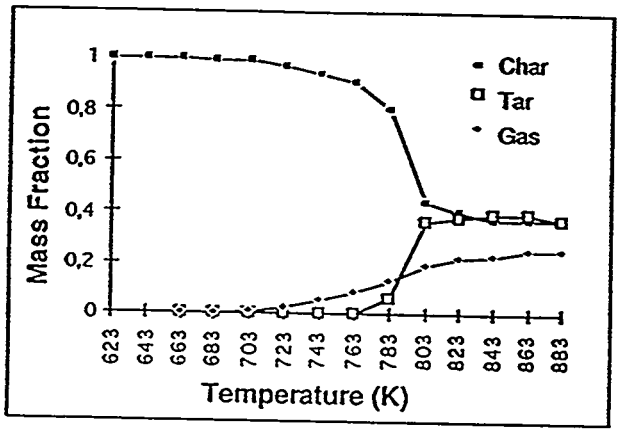

Mc = 4560 amu

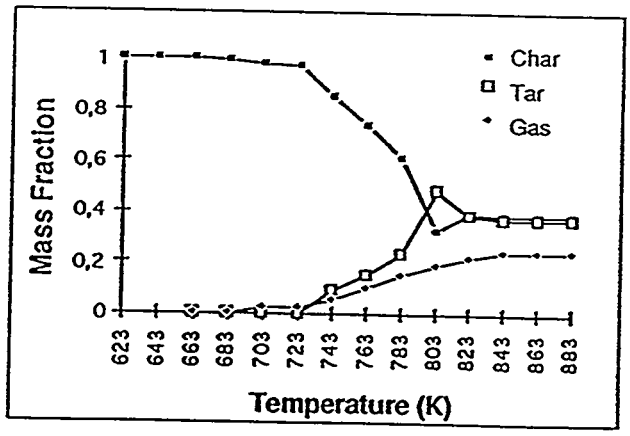

Mc > 4562 amu

igure 8.Simulations of devolatilization yields of char, tar, and light gases versus temperature for arious cross-linked three-dimensional coal models.